

**PHOTOCATALYTIC DEGRADATION OF AZO DYE CONTAMINANT IN  
WASTEWATER USING MESOPOROUS-ASSEMBLED  $\text{In}_2\text{O}_3\text{-TiO}_2$   
MIXED OXIDE PHOTOCATALYSTS**



Siriluck Niyomkarn

A Thesis Submitted in Partial Fulfilment of the Requirements  
for the Degree of Master of Science  
The Petroleum and Petrochemical College, Chulalongkorn University  
in Academic Partnership with  
The University of Michigan, The University of Oklahoma,  
Case Western Reserve University and Institut Français du Pétrole  
2011

I 28375142


**Thesis Title:** Photocatalytic Degradation of Azo Dye Contaminant in Wastewater Using Mesoporous-Assembled  $\text{In}_2\text{O}_3\text{-TiO}_2$  Mixed Oxide Photocatalysts  
**By:** Siriluck Niyomkarn  
**Program:** Petrochemical Technology  
**Thesis Advisors:** Asst. Prof. Thammanoon Sreethawong  
Prof. Sumaeth Chavadej


---


Accepted by the Petroleum and Petrochemical College, Chulalongkorn University, in partial fulfillment of the requirements for the Degree of Master of Science.


  
.....College Dean  
(Asst. Prof. Pomthong Malakul)

**Thesis Committee:**

  
.....  
(Asst. Prof. Thammanoon Sreethawong)

  
.....  
(Prof. Sumaeth Chavadej)

  
.....  
(Asst. Prof. Siriporn Jongpatiwut)

  
.....  
(Dr. Singto Sakulphaemaruehai)

## ABSTRACT

5271034063: Petrochemical Technology Program  
Siriluck Niyomkarn: Photocatalytic Degradation of Azo Dye  
Contaminant in Wastewater Using Mesoporous-Assembled  
In<sub>2</sub>O<sub>3</sub>-TiO<sub>2</sub> Mixed Oxide Photocatalysts  
Thesis Advisors: Asst. Prof. Thammanoon Sreethawong and  
Prof. Sumaeth Chavadej 80 pp.

Keywords: Mesoporous Material/ Photocatalysis/ In<sub>2</sub>O<sub>3</sub>-TiO<sub>2</sub>/ Azo Dye/  
Congo Red/ Degradation

An azo compound is an important class of synthetic dyes and is characterized by the presence of one or more azo group (-N=N-) linked between aromatic rings. The release of this coloring agent causes wastewater problems. Photocatalysis is an efficient technique to remove dye pollutants because of several advantages. This work focused on the improvement of the photocatalytic activity of mesoporous-assembled In<sub>2</sub>O<sub>3</sub>-TiO<sub>2</sub> mixed oxide photocatalysts for Congo Red (CR) azo dye degradation by varying In<sub>2</sub>O<sub>3</sub>-to-TiO<sub>2</sub> molar ratio, calcination temperature, and silver (Ag) loading. All of the photocatalysts were synthesized by a sol-gel process with the aid of a structure-directing surfactant. The experimental results showed that the mesoporous-assembled In<sub>2</sub>O<sub>3</sub>-TiO<sub>2</sub> mixed oxide photocatalyst with an In<sub>2</sub>O<sub>3</sub>-to-TiO<sub>2</sub> molar ratio of 0.05:0.95 calcined at 500 °C provided the highest CR degradation rate constant of 0.86 h<sup>-1</sup>. In addition, the optimum Ag content of 1.5 wt.% loaded on the mesoporous-assembled 0.05In<sub>2</sub>O<sub>3</sub>-0.95TiO<sub>2</sub> photocatalyst by a photochemical deposition method was found to increase the CR degradation rate constant to 1.37 h<sup>-1</sup>.

## บทคัดย่อ

ศิริลักษณ์ นิยมการ : การสลายตัวของสีย้อมประเภทเอโซที่ปนเปื้อนในน้ำเสียโดยใช้ตัวเร่งปฏิกิริยาแบบใช้แสงร่วมประเภทโลหะออกไซด์ผสมระหว่างอินเดียมออกไซด์และไททาเนียที่มีขนาดรูพรุนในระดับเมโซพอร์ (Photocatalytic Degradation of Azo Dye Contaminant in Wastewater Using Mesoporous-Assembled  $\text{In}_2\text{O}_3$ - $\text{TiO}_2$  Mixed Oxide Photocatalysts)  
 อ. ที่ปรึกษา : ผศ. ดร. ธรรมบุญ ศรีทะวงศ์ และ ศ. ดร. สุเมธ ชวเดช 80 หน้า

สีย้อมประเภทเอโซเป็นสารในกลุ่มสีสังเคราะห์ซึ่งประกอบด้วยกลุ่มของเอโซ (-N=N-) ตั้งแต่หนึ่งกลุ่มหรือมากกว่าหนึ่งกลุ่มต่อกับวงสารอะโรมาติกส์ ซึ่งการปล่อยสารพิษประเภทสีย้อมเหล่านี้สู่สภาวะแวดล้อม ก่อให้เกิดปัญหามลพิษในน้ำเสียอย่างหลีกเลี่ยงไม่ได้ การใช้ปฏิกิริยาแบบใช้แสงร่วมเป็นวิธีที่มีประสิทธิภาพวิธีหนึ่งในการกำจัดสารพิษประเภทสีย้อมนี้ เนื่องจากมีข้อดีหลายประการ งานวิจัยนี้จึงมุ่งเน้นศึกษาการปรับปรุงและพัฒนาความสามารถในการย่อยสลายสีย้อมประเภทเอโซชนิดคองโกเรด โดยใช้ตัวเร่งปฏิกิริยาแบบใช้แสงร่วมประเภทโลหะออกไซด์ผสมระหว่างอินเดียมออกไซด์และไททาเนียที่มีขนาดรูพรุนในระดับเมโซพอร์ โดยการเปลี่ยนแปลงตัวแปรต่างๆ ได้แก่ อัตราส่วนโดยโมลของอินเดียมออกไซด์ต่อไททาเนีย, อุณหภูมิที่ใช้ในการเผา, และปริมาณโลหะเงินที่เติมลงบนตัวเร่งปฏิกิริยาแบบใช้แสงร่วมดังกล่าว ในการทดลองนี้ตัวเร่งปฏิกิริยาแบบใช้แสงร่วมถูกสังเคราะห์ขึ้นโดยกระบวนการโซล-เจลร่วมกับการใช้สารลดแรงตึงผิวเป็นตัวกำหนดโครงสร้าง จากผลการทดลองพบว่าตัวเร่งปฏิกิริยาแบบใช้แสงร่วมอินเดียมออกไซด์ไททาเนีย ที่ประกอบด้วยอัตราส่วนโดยโมลของอินเดียมออกไซด์ต่อไททาเนียเท่ากับ 0.05:0.95 ซึ่งถูกเผาที่อุณหภูมิ 500 องศาเซลเซียส ให้ค่าอัตราการย่อยสลายสีย้อมดีที่สุดในที่เท่ากับ 0.86 ต่อชั่วโมง นอกจากนี้การเติมโลหะเงินในปริมาณที่เหมาะสมร้อยละ 1.5 โดยน้ำหนักลงบนตัวเร่งปฏิกิริยาดังกล่าวพบว่า อัตราการย่อยสลายของสีย้อมมีค่าเพิ่มขึ้นเป็น 1.37 ต่อชั่วโมง

## ACKNOWLEDGEMENTS

This thesis work was supported by the Ratchadaphisek Somphot Endowment Fund, the Petroleum and Petrochemical College, and National Center of Excellence for Petroleum, Petrochemicals, and Advanced Materials, Chulalongkorn Thailand.

The author would like to express her sincere gratitude to Asst. Prof. Thammanoon Sreethawong and Prof. Sumaeth Chavadej, her advisors, for their invaluable guidance, understanding, and constant encouragement throughout the course of this research.

She would like to express special thanks to Asst. Prof. Siriporn Jongpatiwut and Dr. Singto Sakulphaemaruthai for kindly serving on her thesis committee. Their sincere suggestions are definitely imperative for accomplishing her thesis.

Her gratitude is absolutely extended to all staffs of the Petroleum and Petrochemical College, Chulalongkorn University, for all their kind assistance and cooperation.

Furthermore, she would like to take this important opportunity to thank all of her graduate friends for their unforgettable friendship.

Finally, she really would like to express her sincere gratitude to her parents and family for the love, understanding, and cheering.

## TABLE OF CONTENTS

	<b>PAGE</b>
Title Page	i
Abstract (in English)	iii
Abstract (in Thai)	iv
Acknowledgements	v
Table of Contents	vi
List of Tables	viii
List of Figures	x
 <b>CHAPTER</b>	
<b>I INTRODUCTION</b>	<b>1</b>
 <b>II LITERATURE REVIEW</b>	
2.1 Azo dyes	4
2.1.1 General Remarks	4
2.1.2 Classification and Designations	4
2.2 Semiconductor	5
2.3 Photocatalysts	7
2.3.1 Titanium Dioxide (TiO <sub>2</sub> )	7
2.3.2 Doping of TiO <sub>2</sub>	10
2.3.3 Indium Oxide and Silver Dopants	11
2.4 Nano-Photocatalysts	14
2.4.1 General Remarks	14
2.4.2 Activity of Nano-Photocatalysts	14
2.5 Photocatalytic Docomposition Mechanisms	15
2.5.1 Photocatalytic Oxidation	15
2.5.2 Photosensitized Oxidation	16
2.6 Factors Influencing Photocatalytic Degradation of Dyes	17
2.6.1 Effect of Initial Dye Concentration	17

<b>CHAPTER</b>	<b>PAGE</b>
2.6.2 Effect of Solution pH	18
2.6.3 Effect of Light Intensity and Irradiation Time	18
2.6.4 Effect of H <sub>2</sub> O <sub>2</sub> Addition	19
2.6.5 Effect of Calcination Temperature of Photocatalyst	20
2.6.6 Effect of Calcination Time of Photocatalyst	20
2.7 Porous Materials	20
2.8 Sol-Gel Process	22
<b>III EXPERIMENTAL</b>	<b>25</b>
3.1 Materials	25
3.2 Equipment	25
3.3 Methodology	26
3.3.1 Synthesis of Mesoporous-Assembled In <sub>2</sub> O <sub>3</sub> -TiO <sub>2</sub> Mixed Oxide Nanocrystal Photocatalysts by a Sol-Gel Process with the Aid of Structure-Directing Surfactant	26
3.3.2 Photocatalyst Characterizations	29
3.3.3 Photocatalytic Experiment	31
<b>IV RESULTS AND DISCUSSION</b>	<b>33</b>
4.1 Photocatalyst Characterizations	33
4.1.1 TG-DTA Results	33
4.1.2 N <sub>2</sub> Adsorption-Desorption Results	35
4.1.3 XRD Results	40
4.1.4 UV-Visible Spectroscopy Results	47
4.1.5 SEM-EDX Results	53
4.1.6 TEM-EDX Results	56
4.1.7 H <sub>2</sub> Chemisorption Results	59

<b>CHAPTER</b>	<b>PAGE</b>
4.2 Photocatalytic CR Dye Degradation Results	60
4.2.1 Effect of In <sub>2</sub> O <sub>3</sub> -to-TiO <sub>2</sub> Molar Ratio in Mixed Oxide Photocatalysts	61
4.2.2 Effect of Calcination Temperature	63
4.2.3 Effect of Ag Loading	65
4.2.4 Effect of Water Hardness	67
4.2.5 Effect of Initial Solution pH	69
<b>V CONCLUSIONS AND RECOMMENDATIONS</b>	<b>72</b>
5.1 Conclusions	72
5.2 Recommendations	73
<b>REFERENCES</b>	<b>74</b>
<b>CURRICULUM VITAE</b>	<b>80</b>



## LIST OF TABLES

TABLE	PAGE	
2.1	Color Index of different azo dyes	5
2.2	The band gap positions of some common semiconductor photocatalysts	7
2.3	Definitions about porous solids	21
4.1	N <sub>2</sub> adsorption-desorption results of the synthesized mesoporous-assembled pure TiO <sub>2</sub> and In <sub>2</sub> O <sub>3</sub> -TiO <sub>2</sub> mixed oxide photocatalysts calcined at various temperatures	39
4.2	N <sub>2</sub> adsorption-desorption results of the synthesized Ag-loaded mesoporous-assembled 0.05In <sub>2</sub> O <sub>3</sub> -0.95TiO <sub>2</sub> mixed oxide photocatalysts calcined at 500 °C	40
4.3	XRD results of the synthesized mesoporous-assembled TiO <sub>2</sub> and In <sub>2</sub> O <sub>3</sub> -TiO <sub>2</sub> mixed oxide photocatalysts calcined at various temperatures	46
4.4	XRD results of the synthesized Ag-loaded mesoporous-assembled 0.05In <sub>2</sub> O <sub>3</sub> -0.95TiO <sub>2</sub> mixed oxide photocatalysts calcined 500 °C	47
4.5	Absorption onset wavelength and band gap energy results of the synthesized mesoporous-assembled pure TiO <sub>2</sub> and In <sub>2</sub> O <sub>3</sub> -TiO <sub>2</sub> mixed oxide photocatalysts calcined at various temperatures	52
4.6	Absorption onset wavelength and band gap energy results of the synthesized Ag-loaded mesoporous-assembled 0.05In <sub>2</sub> O <sub>3</sub> -0.95TiO <sub>2</sub> mixed oxide photocatalysts calcined at 500 °C	53

<b>TABLE</b>	<b>PAGE</b>
4.7 EDX mapping results of the synthesized mesoporous-assembled $0.05\text{In}_2\text{O}_3$ - $0.95\text{TiO}_2$ mixed oxide photocatalyst calcined at 500 °C	56
4.8 Ag dispersion results of the synthesized Ag-loaded mesoporous-assembled $0.05\text{In}_2\text{O}_3$ - $0.95\text{TiO}_2$ mixed oxide photocatalyst calcined at 500 °C	59

## LIST OF FIGURES

FIGURE	PAGE
2.1	The structure of band gap energy. <span style="float: right;">6</span>
2.2	Crystal structures of (a) anatase, (b) rutile, (c) brookite. <span style="float: right;">8</span>
2.3	Mechanism of photocatalysis. <span style="float: right;">10</span>
2.4	A schematic of forming the BaTiO <sub>3</sub> nanoparticles. <span style="float: right;">23</span>
3.1	Synthesis procedure for mesoporous-assembled In <sub>2</sub> O <sub>3</sub> -TiO <sub>2</sub> photocatalysts (a) In <sub>2</sub> O <sub>3</sub> -TiO <sub>2</sub> and (b) Ag-loaded In <sub>2</sub> O <sub>3</sub> -TiO <sub>2</sub> by PCD method. <span style="float: right;">28</span>
3.2	UV light irradiation system for photocatalytic activity test. <span style="float: right;">31</span>
4.1	TG-DTA curves of the dried synthesized photocatalysts: (a) pure TiO <sub>2</sub> and (b) 0.05In <sub>2</sub> O <sub>3</sub> -0.95TiO <sub>2</sub> mixed oxide. <span style="float: right;">34</span>
4.2	N <sub>2</sub> adsorption-desorption isotherms and pore size distributions (inset) of the synthesized mesoporous-assembled photocatalyst calcined at 500 °C: (a) pure TiO <sub>2</sub> , (b) 0.05In <sub>2</sub> O <sub>3</sub> -0.95TiO <sub>2</sub> mixed oxide, and (c) 1.5 wt.% Ag-loaded 0.05In <sub>2</sub> O <sub>3</sub> -0.95TiO <sub>2</sub> mixed oxide. <span style="float: right;">37</span>
4.3	XRD patterns of the synthesized mesoporous-assembled In <sub>2</sub> O <sub>3</sub> -TiO <sub>2</sub> mixed oxide photocatalysts calcined at 500 °C (A = Anatase TiO <sub>2</sub> ). <span style="float: right;">43</span>
4.4	XRD patterns of the synthesized mesoporous-assembled photocatalysts calcined at various temperatures: (a) pure TiO <sub>2</sub> and (b) 0.05In <sub>2</sub> O <sub>3</sub> -0.95TiO <sub>2</sub> mixed oxide (A = Anatase TiO <sub>2</sub> , R = Rutile TiO <sub>2</sub> , I = Rhombic In <sub>2</sub> O <sub>3</sub> ). <span style="float: right;">44</span>
4.5	XRD patterns of the synthesized Ag-loaded mesoporous assembled 0.05In <sub>2</sub> O <sub>3</sub> -0.95TiO <sub>2</sub> mixed oxide photocatalysts calcined at 500 °C (A = Anatase TiO <sub>2</sub> , I = Rhombic In <sub>2</sub> O <sub>3</sub> ). <span style="float: right;">45</span>

FIGURE	PAGE
4.6 UV-visible spectra of the synthesized mesoporous-assembled photocatalysts: (a) pure $\text{TiO}_2$ and $\text{In}_2\text{O}_3$ - $\text{TiO}_2$ mixed oxide calcined at 500 °C, (b) pure $\text{TiO}_2$ calcined at 500-800 °C, (c) $0.05\text{In}_2\text{O}_3$ - $0.95\text{TiO}_2$ mixed oxide calcined at 500-800 °C, and (d) $0.05\text{In}_2\text{O}_3$ - $0.95\text{TiO}_2$ mixed oxide without and with 1.5 wt.% Ag loading calcined at 500 °C.	50
4.7 (a) SEM image and (b) EDX area mappings of the synthesized mesoporous-assembled $0.05\text{In}_2\text{O}_3$ - $0.95\text{TiO}_2$ mixed oxide photocatalyst calcined at 500 °C.	54
4.8 (a) SEM image and (b) EDX area mappings of the synthesized 1.5 wt.% Ag-loaded mesoporous-assembled $0.05\text{In}_2\text{O}_3$ - $0.95\text{TiO}_2$ mixed oxide photocatalyst calcined at 500 °C.	55
4.9 TEM images of the synthesized mesoporous-assembled photocatalysts: (a) pure $\text{TiO}_2$ calcined at 500 °C and, (b, c, d, and e) $0.05\text{In}_2\text{O}_3$ - $0.95\text{TiO}_2$ mixed oxide calcined at 500, 600, 700 and 800 °C, respectively.	57
4.10 TEM image and EDX point mapping of the synthesized 1.5 wt.% Ag-loaded mesoporous-assembled $0.05\text{In}_2\text{O}_3$ - $0.95\text{TiO}_2$ mixed oxide photocatalyst calcined at 500 °C.	58
4.11 UV-visible spectrum of CR dye solution.	60
4.12 Effect of $\text{In}_2\text{O}_3$ -to- $\text{TiO}_2$ molar ratio in terms of $\text{In}_2\text{O}_3$ content of the synthesized mesoporous-assembled $\text{In}_2\text{O}_3$ - $\text{TiO}_2$ mixed oxide photocatalysts calcined at 500 °C on the reaction rate constant for CR dye degradation (Photocatalyst, 0.5 g; total reaction mixture volume, 100 ml; initial CR dye concentration, 200 mg/l; and irradiation time, 4 h).	63

FIGURE	PAGE
4.13 Effect of calcination temperature of the synthesized mesoporous-assembled pure $\text{TiO}_2$ and $0.05\text{In}_2\text{O}_3\text{-}0.95\text{TiO}_2$ mixed oxide photocatalysts on the reaction rate constant for CR dye degradation (Photocatalyst, 0.5 g; total reaction mixture volume, 100 ml; initial CR dye concentration, 200 mg/l; and irradiation time, 4 h).	65
4.14 Effect of Ag loading on the synthesized mesoporous-assembled $0.05\text{In}_2\text{O}_3\text{-}0.95\text{TiO}_2$ mixed oxide photocatalyst calcined at $500\text{ }^\circ\text{C}$ on the reaction rate constant for CR dye degradation (Photocatalyst, 0.5 g; total reaction mixture volume, 100 ml; initial CR dye concentration, 200 mg/l; and irradiation time, 4 h).	67
4.15 Effect of water hardness type and concentration on reaction rate constant for CR dye degradation over the synthesized 1.5 wt.% Ag-loaded mesoporous-assembled $0.05\text{In}_2\text{O}_3\text{-}0.95\text{TiO}_2$ mixed oxide photocatalyst calcined at $500\text{ }^\circ\text{C}$ (Photocatalyst, 0.5 g; total reaction mixture volume, 100 ml; initial CR dye concentration, 200 mg/l; and irradiation time, 4 h).	69
4.16 Effect of initial solution pH on reaction rate constant for CR dye degradation over the synthesized 1.5 wt.% Ag-loaded mesoporous-assembled $0.05\text{In}_2\text{O}_3\text{-}0.95\text{TiO}_2$ mixed oxide photocatalyst calcined at $500\text{ }^\circ\text{C}$ (Photocatalyst, 0.5 g; total reaction mixture volume, 100 ml; initial CR dye concentration, 200 mg/l; and irradiation time, 4 h).	71